Morphology and mechanical behaviour of pea-based starch-protein composites obtained by extrusion

I. Jebalia, J.-E. Maigret, A.-L. Réguerre, B. Novales, S. Guessasma, D. Lourdin, G. Della Valle, Magdalena Kristiawan

▶ **To cite this version:**

I. Jebalia, J.-E. Maigret, A.-L. Réguerre, B. Novales, S. Guessasma, et al.. Morphology and mechanical behaviour of pea-based starch-protein composites obtained by extrusion. Carbohydrate Polymers, 2019, 223, pp.1-9. 10.1016/j.carbpol.2019.115086 . hal-03329262

HAL Id: hal-03329262
https://hal.inrae.fr/hal-03329262v1

Submitted on 26 Oct 2021

HAL is a multi-disciplinary open access archive for the deposit and dissemination of scientific research documents, whether they are published or not. The documents may come from teaching and research institutions in France or abroad, or from public or private research centers.

L'archive ouverte pluridisciplinaire **HAL**, est destinée au dépôt et à la diffusion de documents scientifiques de niveau recherche, publiés ou non, émanant des établissements d'enseignement et de recherche français ou étrangers, des laboratoires publics ou privés.

Distributed under a Creative Commons Attribution - NonCommercial 4.0 International License

Version of Record: https://www.sciencedirect.com/science/article/pii/S0144861719307532
Manuscript_57ca0053d05e9e0d6b25a202ba239f2a

Morphology and mechanical behaviour of pea-based starch-protein composites obtained by extrusion

I. Jebalia, J.-E. Maigret, A.-L. Réguerre, B. Novales, S. Guessasma, D. Lourdin, G. Della Valle, *M. Kristiawan

INRA, UR 1268 Biopolymers Interactions and Assemblies (BIA), 44316 Nantes, France

Authors address e-mail: imen.jebalia@inra.fr
jean-eudes.maigret@inra.fr
anne-laure.reguerre@inra.fr
bruno.novales@inra.fr
sofiane.guessasma@inra.fr
denis.lourdin@inra.fr
guy.della-valle@inra.fr

*Corresponding author: magdalena.kristiawan@inra.fr
Phone: + 33 (0)2 40 67 52 19
Fax: + 33 (0)2 40 67 50 05

Abstract

Starch-legume protein composites were obtained by extrusion of pea flour and pea starch-protein blend at various specific mechanical energies (100-2000 kJ/kg) and a temperature low enough to avoid expansion. The morphology of these composites displayed protein aggregates dispersed in a starch matrix, revealed by microscopy. Image analysis was used to determine the median width of protein aggregates (D_{50}), their total perimeter and surface, from which a protein/starch interface index (I_i) was derived. The mechanical properties of composites were determined by a three-point bending test. The pea flour composites had a higher interface index I_i (1.8-3.1) with lower median particle width D_{50} (8-18 µm) and a more brittle behaviour than the blend composites that had a lower I_i (1-1.1) and higher D_{50} (22-31µm). For both materials, rupture stress and strain were negatively correlated with I_i. This result suggested that there was a poor interfacial adhesion between the pea starch and proteins.

Keywords

Bending test, composite, interface, microstructure, protein aggregates, starch

Abbreviations

a^*	redness in CIELAB colour space
b^*	yellowness in CIELAB colour space
C	torque (N.m)
CLSM	confocal laser scanning microscopy
D_{50}	median protein aggregate width (µm)
db	dry basis
DSC	differential scanning calorimetry
E	flexural modulus (GPa)
F	force (N)

© 2019 published by Elsevier. This manuscript is made available under the CC BY NC user license
https://creativecommons.org/licenses/by-nc/4.0/

H	die thickness (m)
h	specimen width (mm)
I_i	interface index
L^*	lightness in CIELAB colour space
L	support span in bending test (mm)
MC	moisture content (wb)
N	screw speed (rpm)
NF	native pea flour
NSPB	native starch-protein blend
PPI	pea protein isolate
RH	relative humidity (%)
Q	measured total mass flow rate (kg/h)
Q_F	mass flow rate of raw materials (kg/h)
Q_v	volumetric flow rate (m^3/s)
Q_W	mass flow rate of water (kg/h)
SP blend	starch-protein blend
T	product temperature (°C), measured at die entrance
T_{die}	imposed die temperature (°C)
t_h	specimen thickness (°C)
T_m	melting temperature (°C)
T_5	imposed temperature in the fifth barrel (°C)
SME	specific mechanical energy (kJ/kg)
W	die width (m)
wb	wet basis
ΔP	pressure drop inside the die (Pa)
σ	engineering stress (Pa)
ε	engineering strain (%)
η	apparent viscosity (Pa.s)

1. Introduction

Despite their abundance and high nutritional value, pulse legumes (pea, lentil, faba bean, etc.) have not been widely adopted in the human diet. The last decades have been marked by a rising number of research studies in pulse texturisation by extrusion. Low moisture extrusion is often used to produce cereal-based expanded foods whose characteristics owe much to their starch content and macromolecular content. Moreover, supplementation with pulse flour or protein isolates may contribute to the health benefits of these foods thanks to the complementary amino acid profiles of legumes and cereals (Day & Swanson, 2013), while attempting to understand the structural changes of the flour components. During extrusion, after mixing with water, starchy powder becomes molten by solid friction, viscous dissipation and heat conduction from the barrel. The viscous melt is forced through a die where the vapour expands the material to a porous structure, referred to as a solid foam. The texture is governed by density, cellular structure and the mechanical properties of the intrinsic material. The intrinsic material can be envisioned as a dense composite consisting of a blend of starch and protein (Guessasma, Chaunier, Della Valle, &

Lourdin, 2011). In addition to its composition, its mechanical properties depend on the morphology created during extrusion.

High input of thermo-mechanical energy leads to structural modification of the biopolymers, including starch melting and depolymerisation (Logié, Della Valle, Rolland-Sabaté, & Descamps, 2018), protein denaturation and aggregation by non-covalent (hydrophobic) and covalent (disulphide S-S) bonds (Mession, Chihi, Sok, & Saurel, 2015), as well as browning due to Maillard reactions. Shear energy can also favour the unfolding and re-association of protein aggregates (Della Valle, Quillien, & Gueguen, 1994; Fang, Zhang, Wei, & Li, 2013). With increasing melt temperature and specific mechanical energy (*SME*), the starch depolymerisation and its hydrosolubility increase and the protein solubility in the buffer decreases due to protein aggregation by disulphide bonds and increased product browning (Kristiawan et al., 2018).

Most research on the morphology of starch-protein composites has focused on cereal-based systems (Chanvrier, Della Valle, & Lourdin, 2006; Habeych, Dekkers, Goot, & Boom, 2008; Muneer et al., 2016). The effect of protein concentration on the morphology of corn starch-zein composites obtained by extrusion and thermo-moulding was reported by Chanvrier et al. (2006). Habeych et al. (2008) studied the effect of shear rate on the morphology of blends of wheat starch and zein (0-20% db). They found that shear flow changed co-continuous starch-protein morphology into matrix/particle systems with zein aggregates as a dispersed phase. Recently, Kristiawan et al. (2018) showed that the morphology of the intrinsic material of pea flour foams changed from dispersed to bi-continuous system. These changes depended on the structural modifications of biopolymers that were governed by extrusion variables, and temperature in particular. It is therefore necessary to better understand the mechanisms of morphology evolution in legume starch-protein composites.

Several studies have investigated the effect of composition and microstructure (morphology) on the mechanical properties of particulate-biopolymer composites (Chanvrier et al., 2006; Fu, Feng, Lauke, & Mai, 2008; Hashin & Shtrikman, 1962; Leclair & Favis, 1996; Verbeek, 2003). Several empirical or semi-empirical models have been proposed to predict Young's modulus and ultimate strength from composite microstructure, taking the strength of interfacial adhesion, aspect ratio and volume fraction of particles into account (Hashin & Shtrikman, 1962; Nicolais & Nicodemo, 1974; Verbeek, 2003). The mechanical properties of glassy cereal-based starch-protein composites were shown to be weakened by the presence of incompatible dispersed protein aggregates (Chanvrier et al., 2006, Habeych et al., 2008, Muneer et al., 2016). In the case of films of peanut protein isolate blended with pea starch, the decrease of tensile strength and the increase of strain at rupture were attributed to the interaction between swollen pea starch granules and proteins, leading to the formation of a flexible network (Sun, Sun, & Xiong, 2013). To our knowledge, none of the previous studies has determined the relationship between mechanical properties and morphological features of legume composites.

The aim of this work is to determine the relationship between morphological features and mechanical properties for legume composites. To do this, pea flour and a blend of pea starch and pea protein isolate were selected as a model system. The extrusion variables were varied in order to obtain dense composites with a wide variation in starch-protein morphology. The

biopolymer transformations and the morphology and mechanical properties of composites were analysed.

2. Materials and methods

2.1. Raw materials

Yellow pea grits (*Pisum Sativum* L.) were purchased from Sotexpro (France) and ground (SARL Giraud, France) in order to obtain pea flour with a median diameter of 480 µm. Pea starch (amylose content: 35%) and pea protein isolate PPI (Nutralys® F85F) were supplied by Roquettes Frères S.A. (Lestrem, France). The median diameter of pea starch and PPI, determined by laser diffraction (Partica LA-960, HORIBA, Japan) was 27 and 72 µm, respectively. A starch-protein (SP) blend was obtained by mixing pea starch and PPI using a Kenwood mixer for 20 min. The flour and SP blend had a similar ratio of starch and protein: 1.94 and 1.99 dry matter, respectively. The chemical composition of the raw materials (Table1) was determined by standard methods described by Kristiawan et al. (2018).

Table 1. Chemical composition of raw material (% db)

	Starch	Proteins	Ash	Lipids	Others*
Pea starch	98	0.5	0.1	-	1.6
PPI	0.4	88.3	4.5	-	6.8
Pea Flour	46.3	23.9	2.1	2	25.7
Starch-PPI blend	63.3	31.6	1.6	-	3.5

(*) Fibre and other components, determined by difference method (Kristiawan et al., 2018; Li, Kowalski, Li, & Ganjyal, 2016).

2.2. Extrusion

Composites were obtained as strips by extrusion of the pea flour and SP blend using a laboratory scale co-rotating twin-screw extruder (Thermo Scientific™ Process 11, Germany) equipped with a plate die (section: 26 x 1 mm^2; length: 70 mm). The screw diameter was 11 mm and the ratio of length to diameter was 24.5. The barrel was divided into five sections heated separately at 30, 40, 60, 80 and T_5 (92-164) °C. The screw profile included conveying elements with a pitch of 11 mm, followed by four kneading discs (length: 2.75 mm each) that consisted of alternate discs with 0° and 90° on the hexagonal shaft orientation, and one reverse element (length: 5.5 mm) located in the fifth barrel. The die temperature was regulated at 90-95 °C in order to obtain dense composites. The raw material was fed into the first barrel by a volumetric feeder and the water was added to the second barrel using a volumetric pump.

In order to obtain composites with a wide range of starch-protein morphologies and mechanical properties, the operating parameters were varied in the following ranges: moisture content (25-35% wb), screw rotation speed (120-700 rpm) and the temperature of the last barrel of the extruder T_5 (T_m-20 °C, T_m, T_m+20 °C), where T_m is the melting temperature of the raw material. Product pressure and temperature (T) were measured at the die entrance with an accuracy of ± 200 kPa and ± 1 °C, respectively. *SME* (J/g) was calculated as follows:

$$SME = \frac{C.N}{Q} \quad (1)$$

where C is the measured torque (N.m), N the screw speed (rad/s), and Q the mass flow rate (g/s). Apparent viscosity of the melt (η, Pa.s) at the die exit was calculated using Poiseuille's equation through a rectangular channel:

$$\frac{\Delta P}{L} = \frac{12\eta Q_v}{WH^3} \quad (2)$$

where ΔP is the pressure drop inside the die (Pa), Q_v the volumetric flow rate (m^3/s), W the die width (m) and H the die thickness (m).

Immediately after extrusion, the composites were dried at 40 °C for 24 h in order to avoid starch retrogradation and to obtain a final MC of less than 10% wb.

2.3. Starch transformation

Melting transition

In the presence of small amounts of water, as in the case of extrusion ($MC \leq 35\%$ wb), the starch transition is the 'melting' of crystallites in the starch granule. Data for the melting temperature (T_m) of pea flour and the SP blend at various moisture contents is essential to establish the barrel temperature profile (T_5) in order to obtain composites with amorphous starch. T_m values of the SP blend were assumed to be the same as those of pea starch.

Moisture content adjustment was performed by the addition of appropriate quantity of water followed by overnight equilibration or by conditioning pea starch and flour under controlled relative humidity (RH: 58-98%) over saturated salts at 20 °C for one month. The T_m value of native pea starch and flour was determined using a differential scanning calorimetry apparatus Q100 DSC (TA Instruments, USA) according to the method of Logié et al. (2018). The samples were heated from 20 to 200 °C at a heating rate of 5 °C/min. Melting temperature (T_m) was defined as the offset temperature of the melting endothermic peak (Appendix: Fig. A1). The measurements were done in duplicate (relative error: 10%) and were compared to data in the literature (Appendix: Fig. A2).

Crystalline structure

DSC analysis in excess water was performed on the extruded products in order to verify if all starch crystallites were molten by extrusion process. The existence of residual crystalline structure can be indicated by the presence of so-called residual gelatinization endotherm in DSC thermogram. The composites were ground into a fine powder (< 250 µm) using a cryogrinder. The sample (10 mg) and deionised water (40 mg) were directly weighed in a pan and hermetically sealed. The DSC scans were run at 3 °C/min from 20 to 100 °C.

2.4. Colour measurement

The colour of composite surfaces was determined using a Chromameter (Konica Minolta CR-400, France) with a standard D65 illuminant (natural daylight) and an observation angle of 2°. The colour was expressed in CIE-Lab colour space (L^*, a^* and b^*). L^* represents the lightness of colour (0 black, 100 white), a^* and b^* represent the green-red (-100, +100) and blue-yellow (-100, +100) colours, respectively. The reported values were the means of ten measurements (relative error: 10%).

2.5. Morphology

2.5.1. Confocal Laser Scanning Microscopy (CLSM)

The organisation of proteins and starch in pea composites was determined using CLSM.

Sample preparation and labelling

Before cryosectioning, the composites were hydrated by conditioning at 20 °C and *RH* 98% for 4 days, and then cut into pieces of 5 mm in length. For protein labelling, one part (mass) of 0.01% (w/v) fuchsine acid in 1% (v/v) acetic acid was mixed with one part (mass) of Kaiser's glycerol/gelatine solution at 40 °C. Kaiser's solution was used to improve the adhesion of specimen slices on microscope slides (Zweifel, Handschin, Escher, & Conde-Petit, 2003). The specimen slices (thickness: 20 µm) were obtained by cutting the embedded pieces within the freezing medium tissue (Tissue-Tek O.C.T) perpendicularly to the extrusion flow using a cryotome at -20 °C. The slices were mounted in the frozen state onto microscope slides, covered with stained Kaiser's solution and a glass coverslip. The slides were stored for 24 h (20 °C) to insure optimum diffusion of the markers.

Image acquisition

Images were acquired using CLSM (Nikon A1) with an attached NIS imaging system (Nikon, Germany). Samples were examined in the epifluorescence mode of the microscope, excited by a green laser beam at 561 nm. The emitted light was selected by a long-pass filter at 570-620 nm. Images of 512×512 pixels were taken with a magnification of 20 and a resolution of 1.24 µm/pixel.

Image analysis

Image analysis was done for at least three plane projection images of three spots in the composites. It was performed using Matlab software to determine the median particle width (D_{50}), total area and total perimeter of protein aggregates. Firstly, CLSM images were digitised by applying a grey level threshold obtained with a k-mean algorithm (Jain, 2010). The total area of the particles and the total perimeter of their interface with the matrix were then determined. The starch-protein interface index (I_i) was computed as the ratio of the total aggregate perimeter to the square root of the total aggregate area. Granulometry analysis was subsequently performed using mathematical morphology operations (Devaux, Bouchet, Legland, Guillon, & Lahaye, 2008; Le Bleis, Chaunier, Montigaud, & Della Valle, 2016). A curve of the cumulated area of the particles (proteins) was then built according to the width of the openings. This curve was fitted by the Gompertz function (Dehaine & Filippov, 2016):

$$y = c \times exp^{-exp(-k(x-x_c))} \quad (3)$$

where y is the cumulative fraction of particle width less than or equal to the opening width x, c is the amplitude of the cumulative surface (100), k is the constant describing the fragment uniformity, and x_c is the central particle width. The median particle width D_{50} was computed from the Gompertz fit at 50% of the cumulated surface.

2.5.2. Scanning Electron Microscopy

The starch-protein interface of composite materials was ascertained using a scanning electron microscope (JEOL JEM-1230) at an acceleration voltage of 10 kV under low vacuum (100 Pa). Composite samples (1 x 5 x 5 mm^3) were held on specimen holders with transversal cross-sections facing the lens.

2.6. Mechanical properties

Extruded materials were conditioned at a relative humidity of 59% at 20 °C for two weeks in order to obtain a uniform moisture distribution in the material (12±0.5% wb; Appendix: Sorption isotherm measurement, Fig.A3). The mechanical properties of specimen strips (t_h x 100 x 10 mm^3) were determined by a three-point bending test mounted on a dynamometer (Adamel Lhomargy, France). The thickness (t_h) of specimens was measured at three locations with a Vernier caliper. The support span (L) was 40 mm and the crosshead speed was 100 mm/min. The tests were performed until specimens broke. Engineering stress σ (Pa) – strain ε (%) curve was derived from the force–crosshead displacement data as follows:

$$\sigma = \frac{3FL}{2ht_h^2} \quad (4)$$

$$\varepsilon = \frac{6dt_h}{L^2} \quad (5)$$

where F is the force (N), h is the specimen width (0.01 m) and d is the crosshead displacement (m). The stress and strain at rupture corresponded to the maximum of the stress-strain curve. The flexural modulus E (Pa) was defined by the slope of the linear part of the stress-strain curve. The measurements of mechanical properties were performed with ten repetitions, leading to a variability of 20% that mainly due to structural heterogeneity within the specimens.

3. Results

3.1. Extrusion trials

A large interval of *SME* values was obtained (100-2000 kJ/kg), indicating that a wide range of biopolymer changes may be expected (Fig. 1a).

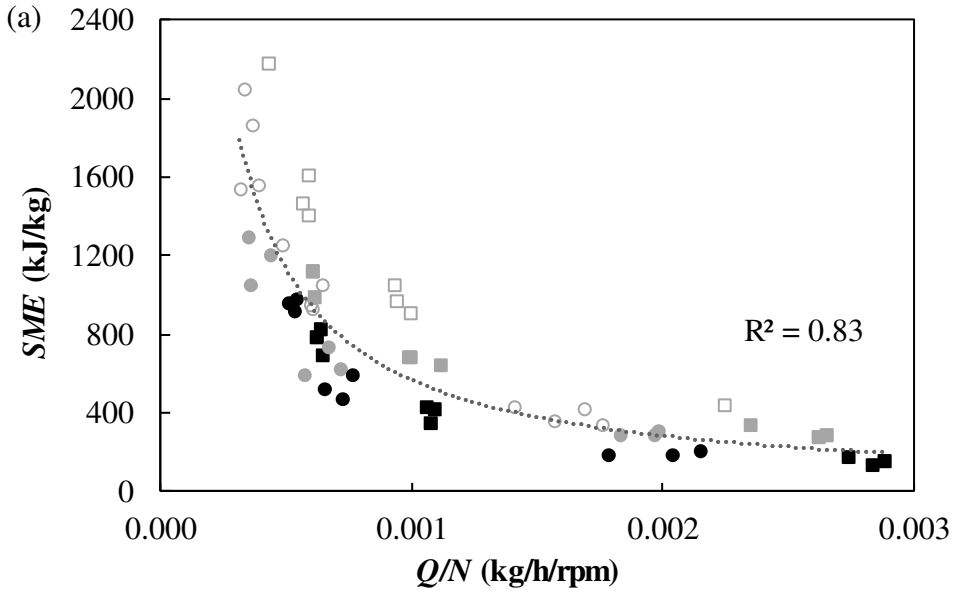

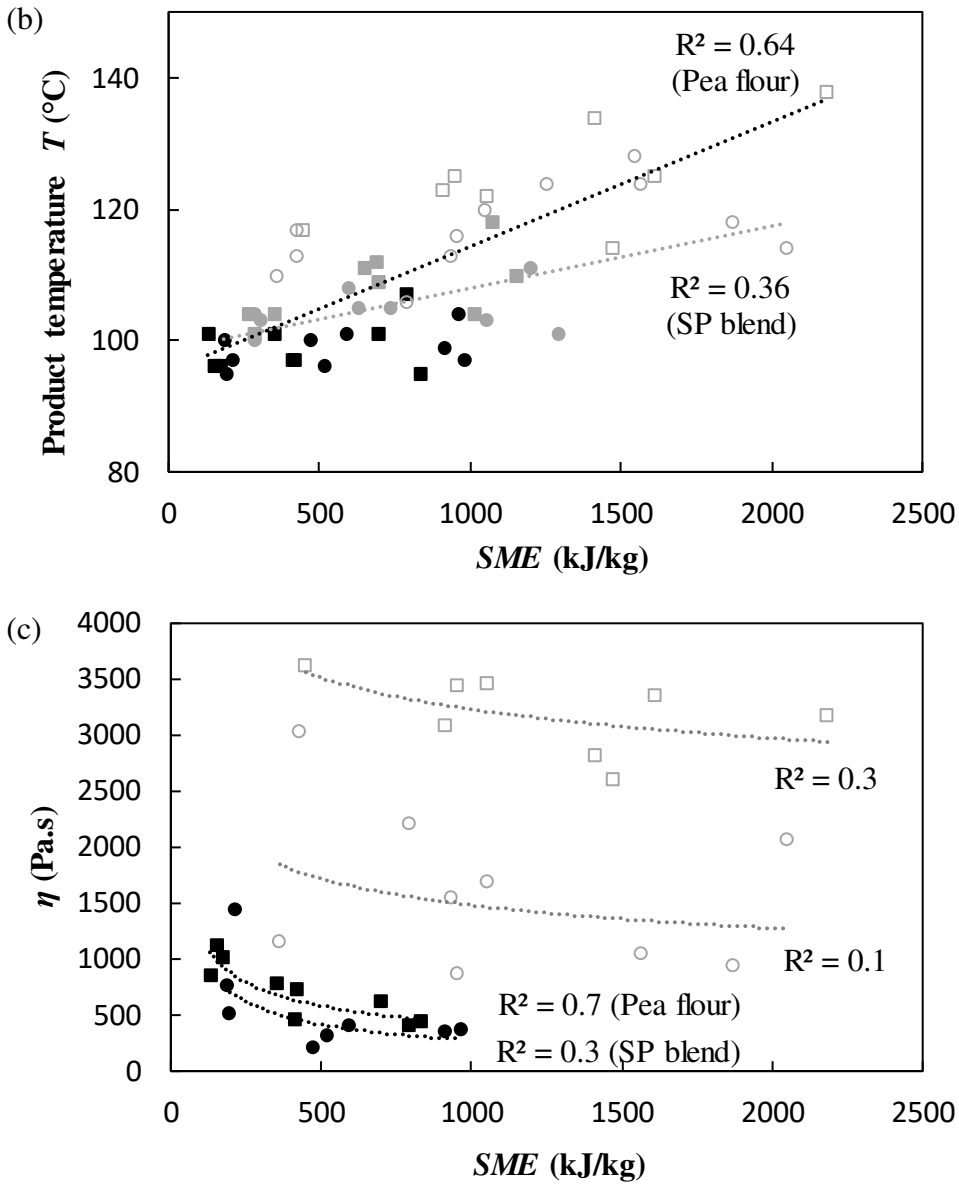

Figure 1. Control of extrusion variables at different moisture contents: 0.25 (white), 0.30 (grey) and 0.35 (black) for pea flour (square) and starch-protein blend (circle): (a) Variation of specific mechanical energy (*SME*) with the ratio of total feed rate (*Q*) to screw speed (*N*), (b) Variation of product temperature (*T*) with *SME,* (c) Variation of melt viscosity (η) with *SME* for moisture contents of 0.25 and 0.35. The dotted line represents data fitting using a power (a, c) and linear (b) function.

SME increased with increasing screw speed and, conversely, decreased when feed rate and moisture content *MC* increased. A negative correlation ($R^2 = 0.83$) between *SME* and the ratio of total feed rate to screw speed (*Q/N*) was obtained for any *MC* and raw material. This result suggested that *SME* can be well controlled by the tuning of these extrusion parameters. Overall, the larger values of *SME* obtained with pea flour might be due to its higher fibre content than that of SP blends (26% versus 3%, in db).

The effect of *SME* on product temperature *T* was positive, regardless of the raw material (Fig. 1b). This trend could be attributed to solid friction between particles and to viscous dissipation in the molten phase, both phenomena explaining why product temperature

is higher than barrel temperature. Higher viscous dissipation suggested that pea flour melt has higher viscosity than that of SP blends, possibly because of its larger fibre content (Fig. 1c).

For all extrusion trials, the melt shear rate maintained the same value (≈ 11±2 s^{-1}) because the total mass flow rate *Q* did not vary much (Table 2). The variations of apparent melt viscosity with *SME* reflected biopolymer structural changes during processing, whereas the dispersion may be attributed to the influence of temperature on viscosity. For instance, it is well known that starch melt viscosity decreases with *SME* because of macromolecular degradation.

Colour and starch changes

The *L** values of extruded composites (Fig. 2) were lower than that of raw materials (*L** 90±1), probably due to Maillard reactions.

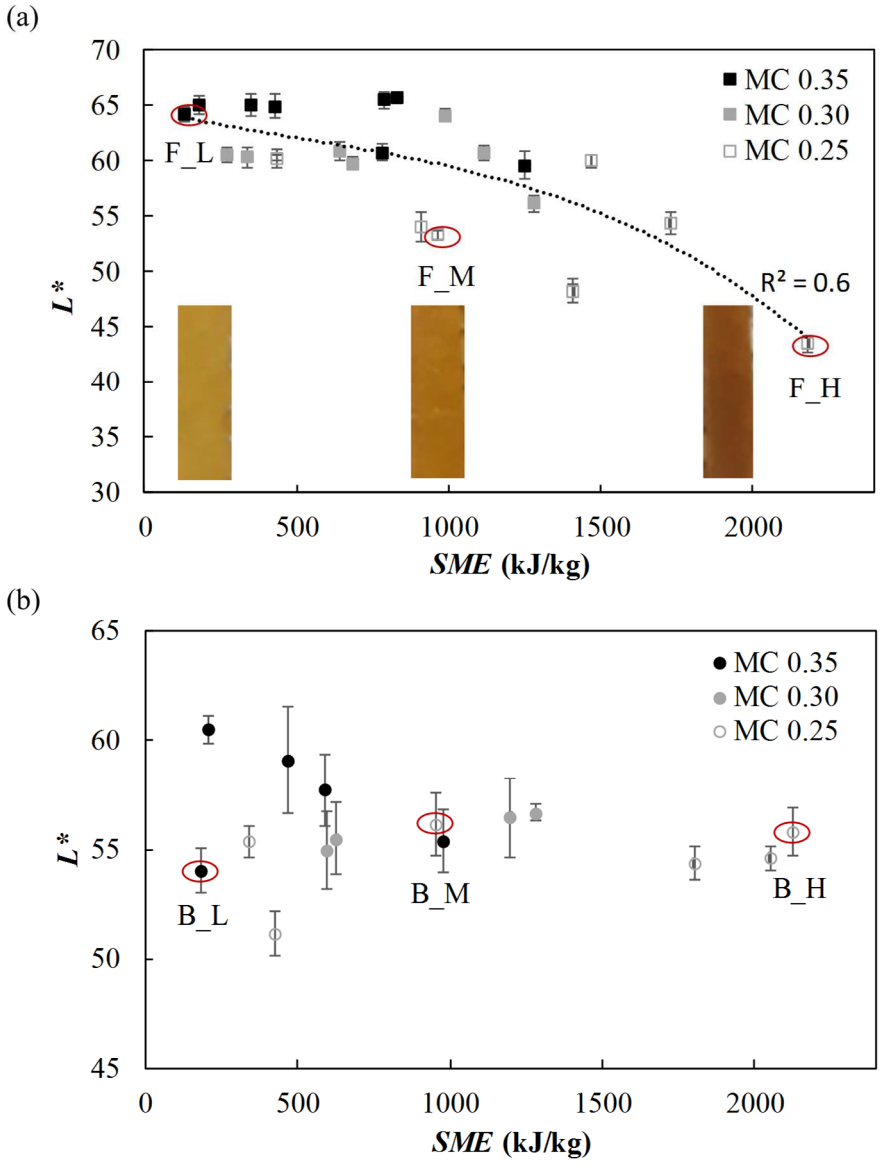

Figure 2. Variation of composite lightness (*L**) of pea flour (a) and the SP blend (b) with specific mechanical energy (*SME*). The L* value of raw materials was 90±1.The symbols refer to data at different extrusion temperatures and the curve represents data fitting using a

third-order polynomial function. The red circles represent the samples selected for further analysis.

Concerning pea flour, the darkness of extruded materials increased with *SME* (R^2 = 0.60) (Fig. 2a). The samples also appeared to be redder (higher a^*, result not shown). No significant L^* colour difference was detected among SP blend composites (L^* = 55±5) (Fig. 2b, ANOVA, p = 0.5, at 5% confidence level).

During extrusion, Maillard reactions occur between protein amino groups and reducing saccharides derived mainly from depolymerised starch. The increased darkness of flour composites at *SME* > 1500 kJ/kg may be due to additional Maillard reactions between proteins and reducing saccharides present in the pea flour fibre (Santillán-Moreno, Martínez-Bustos, Castaño-Tostado, & Amaya-Llano, 2011).

Based on the trend of variation of composite colour with *SME*, three samples of flour composite at different *SME* were selected for further analysis. For the purpose of comparison, three representative composites of SP blend, extruded at similar *SME* levels (≈ 200, 1000, 2000 J/g) were also selected. The name of selected samples was given in Fig. 2 (F: pea flour, B: SP blend; L: low; M: medium; H: high *SME*), and the corresponding extrusion variables were reported in Table 2.

Table 2. Extrusion variables of pea composite

	Operating conditions							Measured variables			
Samples	*MC*	Q_F	Q_w	*N*	T_{die}	T_m	T_5-T_m	*Q*	*T*	*SME*	Die pressure
	% wb	(kg/h)	(kg/h)	(rpm)	(°C)	(°C)	(°C)	(kg/h)	(°C)	(kJ/kg)	(MPa)
Pea flour											
F_L	35	0.24	0.07	120	95	112	20	0.32	101	141	1.2
F_M	25	0.21	0.02	300	95	121	20	0.3	124	1149	7.9
F_H	25	0.21	0.03	650	95	121	0	0.31	138	1952	4
Pea starch-PPI blend											
B_L	35	0.22	0.06	120	90	112	-20	0.33	92	207	3.4
B_M	25	0.24	0.02	300	95	134	20	0.27	134	992	5.7
B_H	25	0.2	0.02	500	95	134	-20	0.26	126	1981	3.5

The starch transformation of selected composites was investigated by comparing their DSC residual gelatinisation enthalpy to the gelatinisation enthalpy of native raw materials (Appendix: Fig. A4). In the excess water (80% wb), the native SP blend and pea flour showed an endothermic transition, reflecting starch gelatinisation, with enthalpies of 5.7 J/g and 3.7 J/g, respectively, at the same peak temperature (69-70 °C). No residual gelatinisation enthalpy was detected for the selected composites, indicating complete melting of starch crystals during extrusion. Therefore, for all extruded composites, starch was considered amorphous.

3.2. Morphology

The organisation of starch and proteins of raw material and selected composites was investigated using CLSM and presented in Figs. 3a, b and c. The grey areas correspond to the starch phase and the green areas depict the protein phase.

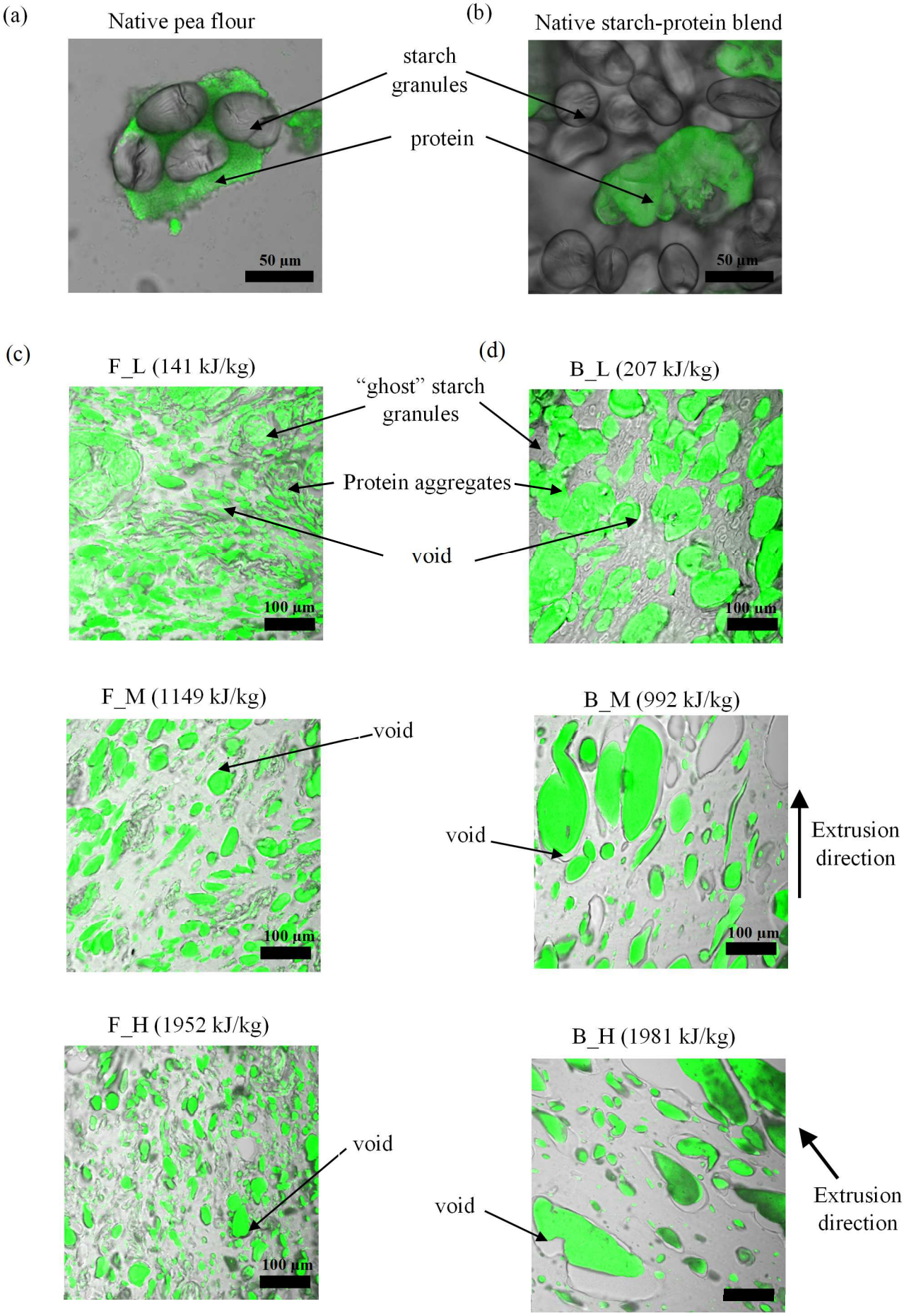

Figure 3. The morphology of raw material and composites observed by CLSM:

- Starch granules and protein bodies in raw pea flour (a) and starch-protein SP blend (b).
- Amorphous starch and protein aggregates in pea flour (c) and SP blend (d) composites extruded at three levels of *SME*. The sample B_H was slightly rotated on the microscopic slide.

The proteins were stained green with fuchsin acid. Unstained amorphous starch was in grey. The white space at the interface of starch and protein aggregates indicated the void.

Image description

In native pea flour, proteins surrounded starch granules, whereas proteins formed an independent structure in native SP blends (Fig. 3a). In all composites, the morphology showed protein aggregates dispersed in a continuous matrix of amorphous starch for various *SME* values (Figs. 3b, c). Chanvrier et al. (2006) also observed similar morphology, namely matrix-particle, for thermo-moulded or extruded corn flour and starch-zein blends, when zein concentration was lower than 20% (db). They suggested that the protein aggregates derived from the protein bodies were disrupted, denatured and cross-linked due to high mechanical energy and temperature. In our case, protein aggregates observed in SP blend composites were clearly larger than in flour composites, likely due to the wet extraction process of PPI that results in assembled protein particles (Fig. 3b). For both composites, starch and protein domains were separated by voids, as precisely observed by scanning electron microscopy (Fig. 4).

These voids can result from interfacial debonding during melt cooling after leaving the extruder die, as well as from sample cryosectioning for microscopy analysis. The interface voids indicating poor interfacial adhesion were also observed for starch-zein blend composites formed by simple shear flow (Habeych et al., 2008). Utracki (2002) reported that the presence of voids in polymer blends was due to poor compatibility of the phases. Hence, regardless of the explanation, it is likely that composite morphology is due to poor adhesion of starch and proteins in the glassy domain.

The CLSM images showed that the size and shape of protein aggregates was not uniform within composites, and this non-uniformity was more marked in SP blend composites than in those of flour. The composites extruded at *SME* < 200 kJ/kg (F_L, B_L) exhibited the highest protein area. Protein aggregates in flour composites did not present any orientation, whereas they were oriented in the extrusion direction in SP blend composites extruded at *SME* $\geq$ 1000 J/g (B_M, B_H). Starch granules were transformed into a homogenous matrix of amorphous starch with the exception of F_L and B_L composites. Indeed, these composites presented deformed ghost starch granules (size ≈ 22 mm) that were entrapped by proteins in F_L, and were dispersed and elongated in continuous phase in B_L. Similar flour composite morphology was observed by Kristiawan et al. (2018) in the intrinsic material of expanded pea flour. These observations clearly revealed that the variation of extrusion variables (*SME)* led to various composite morphologies, which required morphological analysis for further quantification.

The total area of protein aggregates decreased from 130 to 80 mm^2 with increasing *SME* ($R^2 = 0.97$; Fig. 5a). This result may be attributed to the increase in starch transformation with *SME*, reflected, for instance, by the increase in water swelling (Kristiawan et al., 2018). These changes would cause the starch to swell up and disperse more easily, leading to a larger area of the continuous phase at the expense of the dispersed phase, protein aggregates in this case.

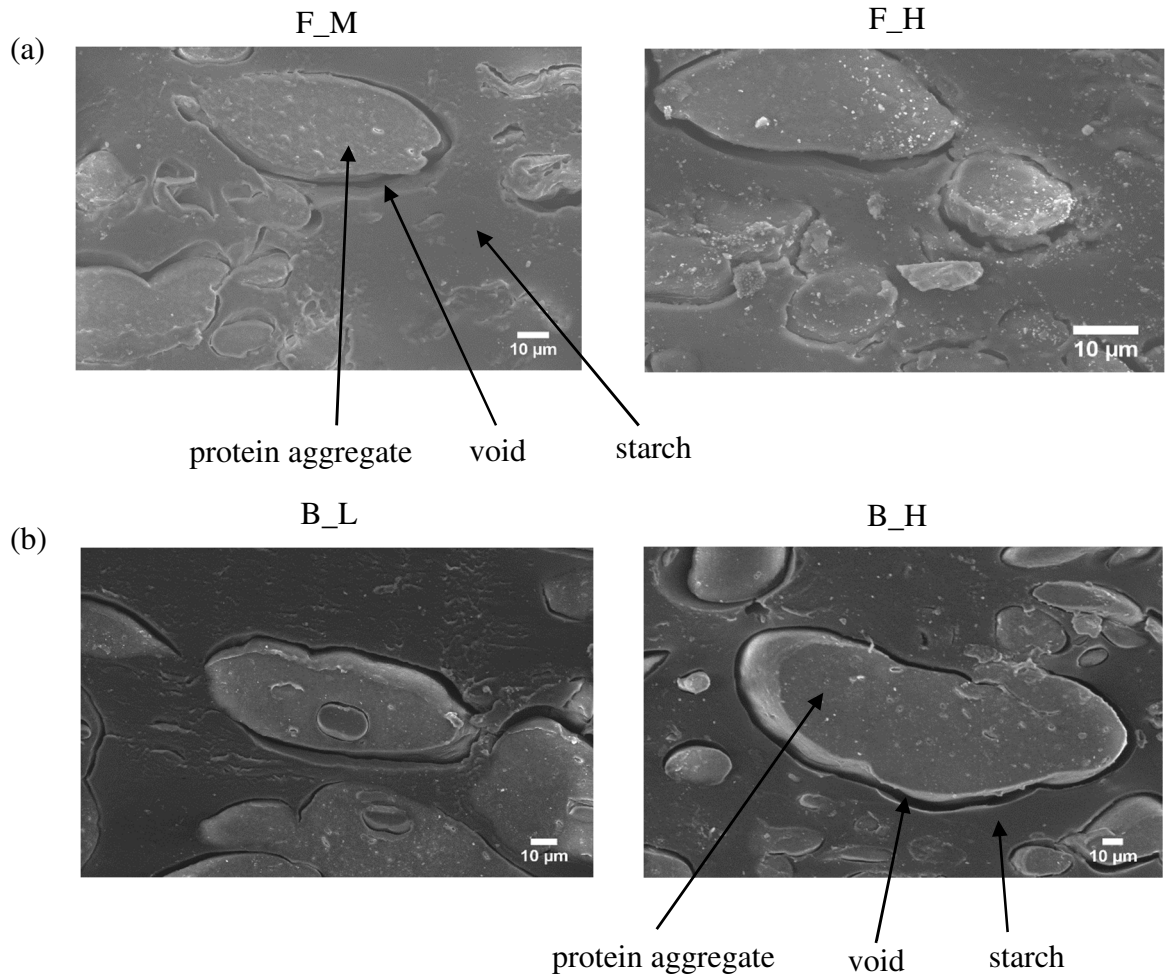

Figure 4. Scanning electron microscope images of pea flour (a) and starch-protein blend (b) composites. Voids were observed at the interface of amorphous starch and protein aggregates.

Image analysis

The distribution curves of the width of protein aggregates were presented as the cumulated percentage of the total area occupied by aggregates (Fig. 5b). The good curve fitting by the Gompertz function allowed accurate determination of median aggregate size (D_{50}). The SP blend composites presented larger protein aggregates (D_{50} = 22-31 µm) than flour composites (D_{50} = 8-18 µm). The relative standard deviation of D_{50} values was between 11 and 15% for all samples, except for B_L that was 28%.

The interface index (I_i) of pea flour composite, defined as the ratio of the total aggregate perimeter to the square root of the total aggregate area, varied from 3 to 1, the lower value being obtained for SP blend composites. Not surprisingly, it was strongly and negatively correlated with D_{50} (R^2 = 0.93): the smaller the aggregates were, the larger the relative interface between proteins and starch was (Fig. 5c). This result confirms the qualitative trend observed from CLSM images (Fig. 3): many small protein aggregates (F_L) have a larger total perimeter than a few large and sparse aggregates (B_H). Since both features, interface index and median width are correlated, the following results will be compared using only I_i.

(a)

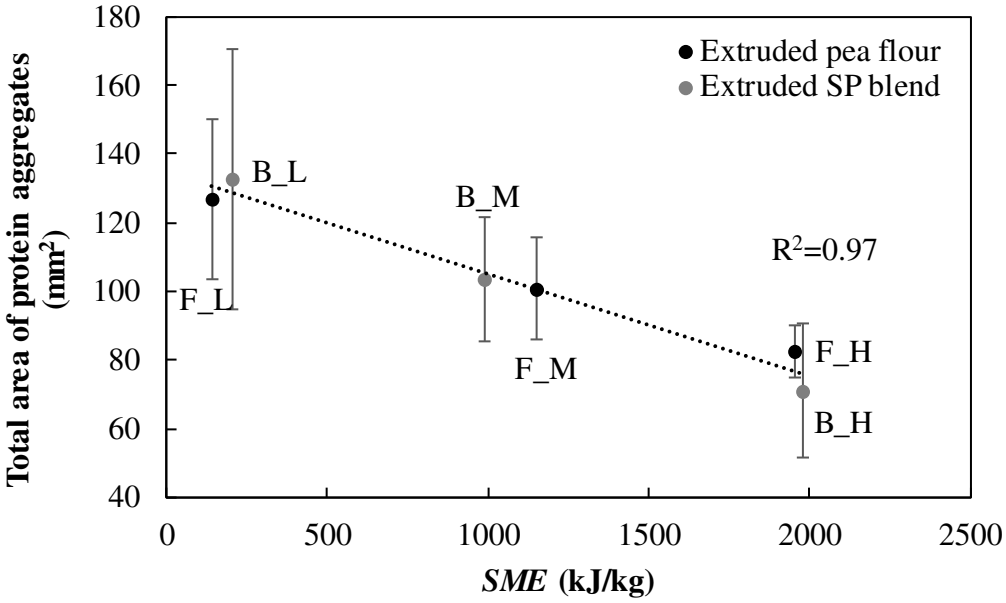

391

(b)

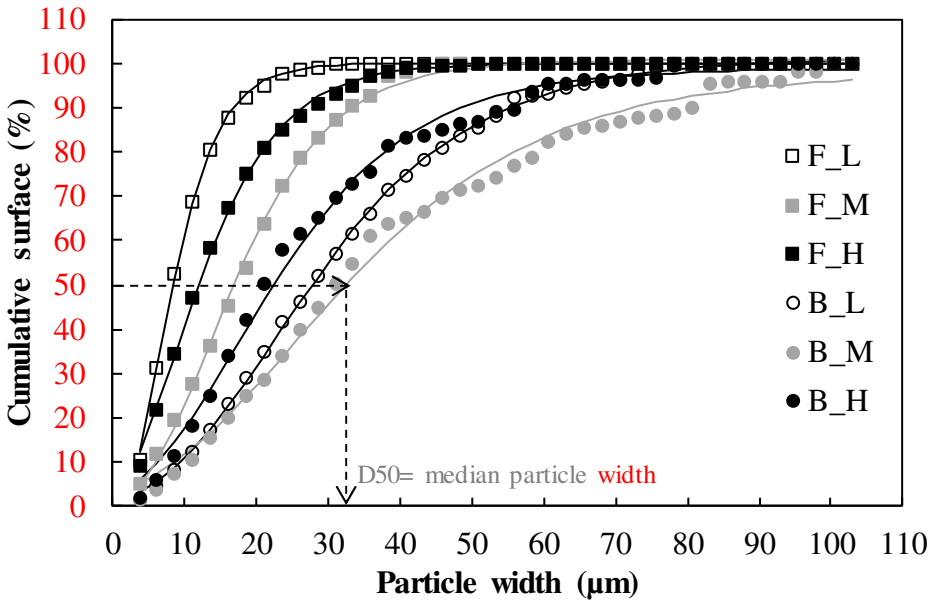

392

(c)

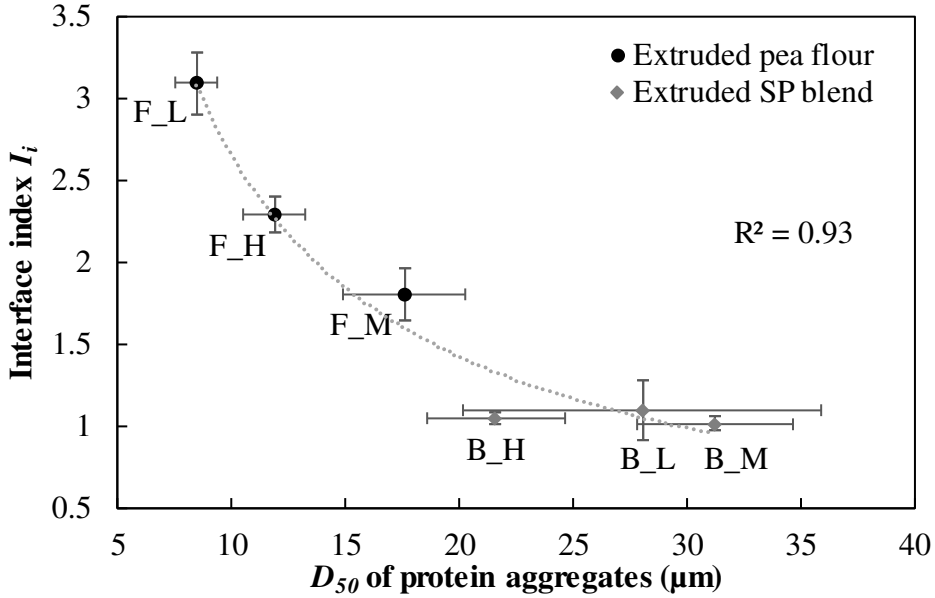

393
394

(d)

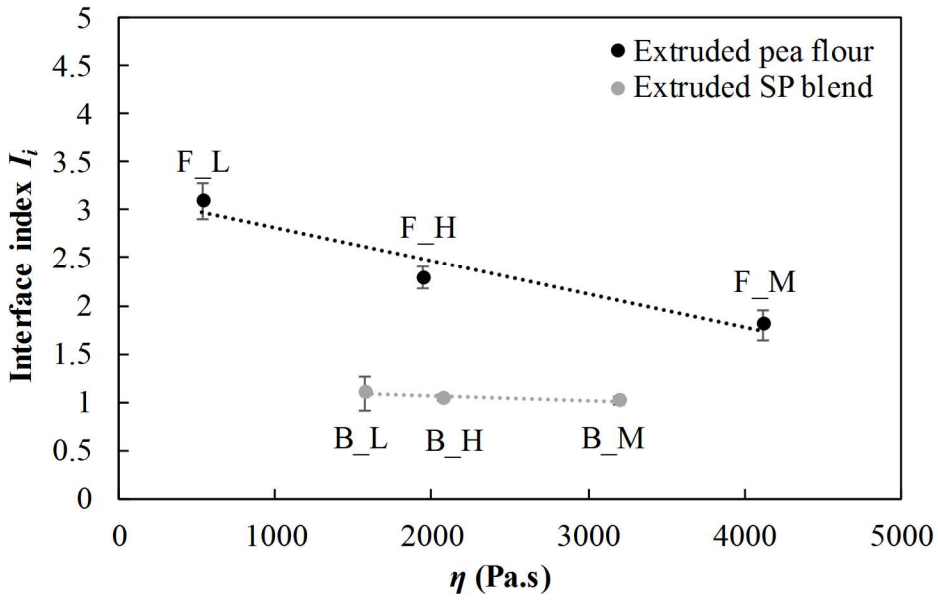

Figure 5. Variations of composite morphology features: total area of protein aggregates with specific mechanical energy (*SME*) (a); cumulative distribution of protein aggregate width for pea flour (square) and starch-protein blend (circle) composites (b); solid lines represent data fitting using the Gompertz function (Eq. 3, $R^2 > 0.98$); interface index I_i with median protein aggregate width D_{50} (c); interface index I_i with apparent viscosity η (d). The dotted lines represent the data fitting using appropriate mathematical, polynomial or power functions.

The interface index decreased slightly with the apparent viscosity η (Fig. 5d). This variation is tiny and even not significant in the case of SP blends, given the large variation of viscosity. Conversely, during shear flow, viscosity is expected to increase with interface because of interfacial effects between the molten phases, as suggested for starch-zein blends (Chanvrier, Chaunier, Della Valle, & Lourdin, 2015). Hence, this result suggests that other structural changes, possibly antagonistic, like fragmentation of protein aggregates or starch degradation prevail in the building of the composite morphology.

3.3. Mechanical properties

The main results of the three-point bending test of composites (*MC* 12% wb, 20 °C) are illustrated in Fig. 6. Stress-strain curves revealed that flour composites exhibited brittle behaviour with the rupture of specimens in the elastic domain. SP blend composites were less brittle because their rupture took place beyond the elasticity stage. At similar *SME,* SP blend composites had higher values of stress and strain at rupture and lower values of flexural modulus than flour composites (Table 3).

The rupture stress of pea composites was in the range of extruded and thermo-moulded corn flour (18 MPa) and starch-zein composites (~25 MPa) (Chanvrier, Chaunier, Della Valle, & Lourdin, 2015; Chanvrier, Colonna, Della Valle, & Lourdin, 2005). The higher fibre content of pea flour (26% db) may partly explain the difference in the mechanical behaviour of the composites (Muneer et al., 2018). According to Robin, Dubois, Curti, Schuchmann, & Palzer (2011), the rupture could occur either by fibre fracture or by fracture at the interface of fibre and continuous starch.

The flexural modulus was found to be independent of morphological characteristics (Appendix: Fig. A5). Chanvrier et al. (2016) reported that zein content had no significant effect on the storage modulus of starch-zein composites at room temperature. This may be due to close values of the storage modulus of glassy starch and proteins. The mechanical properties were defined only by stress and strain at the rupture point.

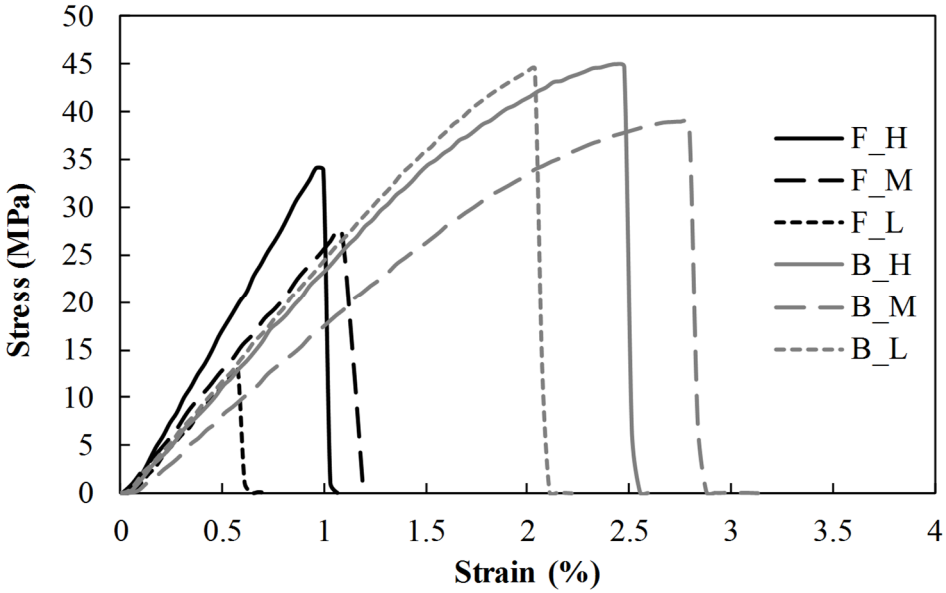

Figure 6. Engineering stress-strain curve obtained by a 3-point bending test for pea flour (black lines) and starch-protein blend (grey lines) composites (20 °C, MC 12 ± 0.5% wb).

Table 3. Morphological features and mechanical properties of pea composite

Samples	Morphological features			Mechanical properties		
	Total area (mm^2)	D_{50} (µm)	I_i	$\sigma_{rupture}$ (MPa)	$\varepsilon_{rupture}$ (%)	E (GPa)
			Pea flour			
F_L	127±23	8±1	3.1±0.2	15±2	0.8±0.3	2±0.6
F_M	101±15	18±3	1.8±0.2	25±5	1.1±0.3	2.4±0.5
F_H	82±8	12±1	2.3±0.1	30±7	1±0.2	3.1±0.5
			Pea starch-PPI blend			
B_L	133±38	28±8	1.1±0.2	44±5	2.1±0.2	2.4±0.2
B_M	104±18	31±3	1±0.04	40±2	2.8±0.4	1.9±0.1
B_H	71±19	22±3	1±0.04	46±2	2.5±0.1	2.4±0.1

The interface index (I_i) negatively influenced the composite breaking stress and strain ($R^2 \approx 0.90$; Fig. 7). This result can be explained by the poor interfacial adhesion between the starch matrix and protein aggregates, as suggested from microscopy images. The larger I_i was, the higher the interfacial debonding created under stress and the more brittle the composite were. The strength of composites strongly depends on the stress transfer between the particles and matrix (Fu et al., 2008). For a poorly bonded particle/matrix, the stress transfer at the interface was inefficient. As shown in Fig. 5c, the flour composites had smaller D_{50} and larger

I_i than SP composites. Combined with less effective stress transfer mechanisms, these factors made flour composites more brittle than those of SP blends.

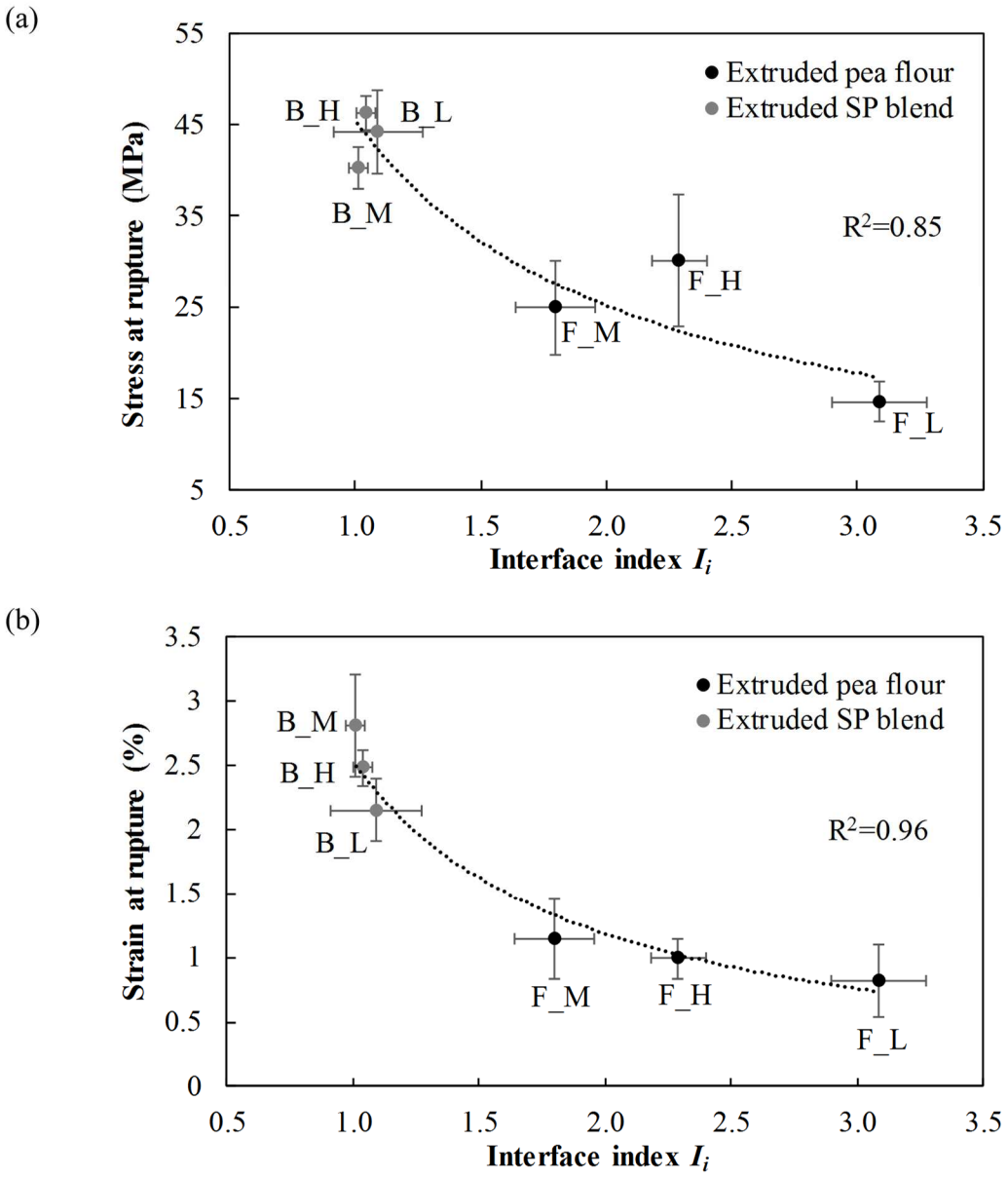

Figure 7. Effect of the interface index on stress (a) and strain (b) at rupture. The dotted lines represent data fitting using power functions.

In the field of polymer/material science, it is assumed that the incorporation of micro- and nanoparticles reinforces composite mechanical properties, i.e., increases Young's modulus, breaking strength and fracture toughness. The challenge for the food sciences is the opposite. Increased brittleness of extruded foods is considered to be advantageous for chewing and nutrient release during digestion. Expanded leguminous snacks, obtained by extrusion, were distinguished by uniform and relatively small pore structure (Li et al., 2016). For the same density, starch foams with a fine cellular structure were found to be more resistant to rupture than coarser structures (Babin, Della Valle, Dendievel, Lourdin, & Salvo,

2007). A fine cellular structure with crispy texture can be obtained by controlling the fragility of cell walls, which depends on starch-protein morphology, i.e., interface index and strength of interfacial adhesion. In turn, morphology can be controlled by tuning the extrusion variables (*SME*) and formulation.

Conclusions

Pea composites were obtained by extrusion in a large interval of *SME* which was particularly tuned by the ratio of total flow rate to screw speed. Different morphologies were obtained by modifying the *SME*. The structure of pea flour and starch-protein (SP) blend composites consisted generally of dispersed protein aggregates in an amorphous starch matrix. The presence of voids between the phases indicated poor interfacial adhesion. The total area of protein aggregates decreased with increasing *SME* due to starch swelling leading to larger area of the continuous phase (starch) at the expense of dispersed protein aggregate. Pea flour composites exhibited brittle behaviour with rupture in the elastic domain, whereas SP blend composites exhibited higher breaking stress and strain with rupture in the plasticity stage. The interface index, which was defined as the ratio of the aggregate perimeter to the square root of the total aggregate area, explained the variation of mechanical properties, regardless of the composite formulation. Increasing the interface index with poor compatibility between the phases weakened the composites. Finally, it is possible to modulate the mechanical properties by tuning the composite morphology through extrusion variables. These results will contribute to the determination of constitutive laws of starch-protein composites. These laws will be integrated into multi-scale numerical models to predict the mechanical properties of solid foams based on knowledge of the cellular structure and morphology of intrinsic material.

Acknowledgements

The authors are grateful to K. Cahier and R. Desirest for technical assistance. This work was supported by the Pays de la Loire Region (France) and INRA (Institut National de la Recherche Agronomique).

Appendix

Supplementary material related to this article can be found in the online version.

References

Babin, P., Della Valle, G., Dendievel, R., Lourdin, D., & Salvo, L. (2007). X-ray tomography study of the cellular structure of extruded starches and its relations with expansion phenomenon and foam mechanical properties. *Carbohydrate Polymers*, *68*, 329–340.

Chanvrier, H., Chaunier, L., Della Valle, G., & Lourdin, D. (2015). Flow and foam properties of extruded maize flour and its biopolymer blends expanded by microwave. *Food Research International*, *76*, 567–575.

Chanvrier, H., Colonna, P., Della Valle, G., & Lourdin, D. (2005). Structure and mechanical behaviour of corn flour and starch-zein based materials in the glassy state. *Carbohydrate Polymers*, *59*, 109–119.

Chanvrier, H., Della Valle, G., & Lourdin, D. (2006). Mechanical behaviour of corn flour and starch-zein based materials in the glassy state: A matrix-particle interpretation. *Carbohydrate Polymers*, *65*, 346–356.

Day, L., & Swanson, B. G. (2013). Functionality of protein-fortified extrudates. *Comprehensive Reviews in Food Science and Food Safety*, *12*, 546–564.

Dehaine, Q., & Filippov, L. O. (2016). Modelling heavy and gangue mineral size recovery curves using the spiral concentration of heavy minerals from kaolin residues. *Powder Technology*, *292*, 331–341.

Della Valle, G., Quillien, L., & Gueguen, J. (1994). Relationships between processing conditions and starch and protein modifications during extrusion-cooking of pea flour. *Journal of the Science of Food and Agriculture*, *64*, 509–517.

Devaux, M.-F., Bouchet, B., Legland, D., Guillon, F., & Lahaye, M. (2008). Macro-vision and grey level granulometry for quantification of tomato pericarp structure. *Postharvest Biology and Technology*, *47*, 199–209.

Fang, Y., Zhang, B., Wei, Y., & Li, S. (2013). Effects of specific mechanical energy on soy protein aggregation during extrusion process studied by size exclusion chromatography coupled with multi-angle laser light scattering. *Journal of Food Engineering*, *115*, 220–225.

Fu, S., Feng, X., Lauke, B., & Mai, Y. (2008). Effects of particle size, particle/matrix interface adhesion and particle loading on mechanical properties of particulate–polymer composites. *Composites: Part B*, *39*, 933–961.

Guessasma, S., Chaunier, L., Della Valle, G., & Lourdin, D. (2011). Mechanical modelling of cereal solid foods. *Trends in Food Science and Technology*, *22*, 142–153.

Habeych, E., Dekkers, B., Goot, A. J. Van Der, & Boom, R. (2008). Starch-zein blends formed by shear flow. *Chemical Engineering Science*, *63*, 5229–5238.

Hashin, Z., & Shtrikman, S. (1962). On some variational principles in anisotropic and nonhomogeneous elasticity. *Journal of the Mechanics and Physics of Solids*, *10*, 335–342.

Jain, A. K. (2010). Data clustering : 50 years beyond K-means. *Pattern Recognition Letters*, *31*, 651–666.

Kristiawan, M., Micard, V., Maladira, P., Alchamieh, C., Maigret, J.-E., Réguerre, A.-L., Amin, M.A., Della Valle, G. (2018). Multi-scale structural changes of starch and proteins during pea flour extrusion. *Food Research International*, *108*, 203–215.

Le Bleis, F., Chaunier, L., Montigaud, P., & Della Valle, G. (2016). Destructuration mechanisms of bread enriched with fibers during mastication. *Food Research International*, *80*, 1–11.

Leclair, A., & Favis, B. D. (1996). The role of interfacial contact in immiscible binary polymer blends and its influence on mechanical properties. *Polymer*, *37*, 4723–4728.

Li, C., Kowalski, R. J., Li, L., & Ganjyal, G. M. (2016). Extrusion expansion characteristics of samples of select varieties of whole yellow and green dry pea flours. *Cereal Chemistry Journal*, *94*, 385–391.

Mession, J. L., Chihi, M. L., Sok, N., & Saurel, R. (2015). Effect of globular pea proteins fractionation on their heat-induced aggregation and acid cold-set gelation. *Food Hydrocolloids*, *46*, 233–243.

538 Muneer, F., Andersson, M., Koch, K., Hedenqvist, M. S., Gaallstedt, M., Plivelic, T. S.,
539 Menzel, C., Rhazi, L., & Kuktaite, R. (2016). Innovative gliadin/glutenin and modified
540 potato starch green composites : Chemistry, structure and functionality induced by
541 processing. *ACS Sustainable Chemistry & Engineering*, *4*, 6332–6343.

542 Muneer, F., Johansson, E., Hedenqvist, M. S., Plivelic, T. S., Markedal, K. E., Petersen, I. L.,
543 Sørensen, J., C, & Kuktaite, R. (2018). The impact of newly produced protein and
544 dietary fiber rich fractions of yellow pea (*Pisum sativum* L.) on the structure and
545 mechanical properties of pasta-like sheets. *Food Research International*, *106*, 607–618.

546 Nicolais, L., & Nicodemo, L. (1974). The effect of particles shape on tensile properties of
547 glassy thermoplastic composites. *International Journal of Polymeric Materials*, *4*, 229-
548 243.

549 Robin, F., Dubois, C., Curti, D., Schuchmann, H. P., & Palzer, S. (2011). Effect of wheat bran
550 on the mechanical properties of extruded starchy foams. *Food Research International*,
551 *44, 2880-2888.*

552 Santillán-Moreno, A., Martínez-Bustos, F., Castaño-Tostado, E., & Amaya-Llano, S. L.
553 (2011). Physicochemical characterization of extruded blends of corn starch-whey protein
554 concentrate–*Agave tequilana* fiber. *Food and Bioprocess Technology*, *4*, 797–808.

555 Sun, Q., Sun, C., & Xiong, L. (2013). Mechanical, barrier and morphological properties of
556 pea starch and peanut protein isolate blend films. *Carbohydrate Polymers*, *98*, 630–637.

557 Verbeek, C. J. R. (2003). The influence of interfacial adhesion, particle size and size
558 distribution on the predicted mechanical properties of particulate thermoplastic
559 composites. *Materials Letters*, *57*, 1919–1924.

560 Zweifel, C., Handschin, S., Escher, F., & Conde-Petit, B. (2003). Influence of high-
561 temperature drying on structural and textural properties of durum wheat pasta. *Cereal*
562 *Chemistry*, *80*, 159–167.